EXAMENSARBETE I GEOLOGI VID LUNDS UNIVERSITET

Mineralogi och petrologi

Modelling Mössbauer spectra of biotite

Jonas Bermin

Lund 2001 Examensarbete, 20 p Nr 142
Geologiska Institutionen, Lunds Universitet

CODEN: SE-LUNBDS/NBGO-01/5142+21s

EXAMENSARBETE I GEOLOGI VID LUNDS UNIVERSITET

Mineralogi och petrologi

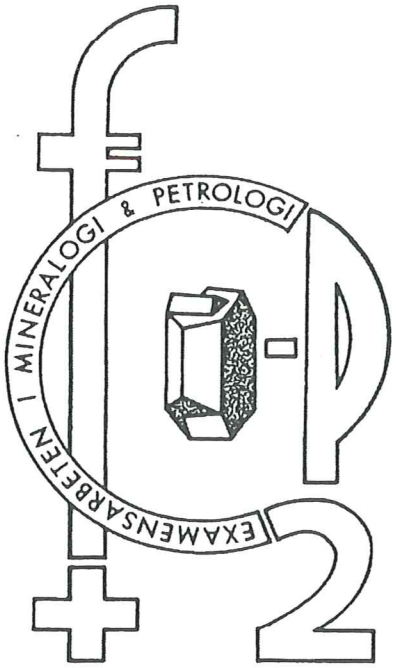

Modelling Mössbauer spectra of biotite

Jonas Bermin

Lund 2001 Examensarbete, 20 p Nr 142
Geologiska Institutionen, Lunds Universitet

Contents

Modelling Mössbauer spectra of biotite

Jonas Bermin

Bermin, J., 2001: Modelling Mössbauer spectra of biotite. *Examensarbete i geologi vid Lunds Universitet. 20 poäng.*

Abstract

The Mössbauer effect is used in this work to determine the oxidation and site occupation in biotites that have been treated in different pHs. The work also gives an introduction to the theory behind the Mössbauer effect as well as Mössbauer spectroscopy.

It is obvious that the pH has a significant role in the oxidation of the biotites, the more acidic the sample the more it will be oxidised. It is also clear from this study that of the two different sites in the octahedral positions it is the M2, or the cis-position, that is the one that is easier to oxidise. These statements require that the models used to fit the spectra are accurate. This work gives a brief model comparison between two well-used methods, the Lorentzian line doublets and the QSD's. This comparison together with comments from other writers suggested that the QSD model would be the best one to use. The model gives good data on the oxidation state but the data given from the M1, M2 occupation isn't as good. This problem is however common for any model studying biotites. A short comparison to the Mössbauer spectra of Muscovite, a mineral similar in chemistry and structure, to biotite, is given because of the difference between the spectra of the two minerals. Muscovite shows easy separation between the two M1, M2 sites while biotite doesn't. The reason to this difference is probably dependent on the chemical differences and the differences in distortion between the sites of the two minerals.

Jonas Bermin, Department of Geology, Sub department of Mineralogy and Petrology, Sölvegatan 13, S-223 62 Lund, Sverige

Modellering av Mössbauerspektra för biotit

Jonas Bermin

Bermin, J., 2001: Modelling Mössbauer spectra of biotite. *Examensarbete i geologi vid Lunds Universitet. 20 poäng.*

Abstract

Mössbauer-effekten används i detta arbete för att bestämma oxidationsgrad och plats besättning i biotiter som har blivit behandlade vid olika pH. Arbetet ger också en introduktion till teorin bakom Mössbauer-effekten samt till Mössbauer-spektroskopi.

Det är tydligt att pH har en viktig roll i oxidationen av biotiter, ju surare prov desto mer kommer det att oxideras. Det är också klart från det här arbetet att av de två oktagon positionerna är det M2, eller cis-positionen som oxideras lättast. Dessa uttalanden kräver att modellen som används för att passa spektrumen är korrekt. Detta arbete ger en kort modell jämförelse mellan två ofta använda metoder, Lorentzian dubbletter och QSD. Denna jämförelse tillsammans med kommentarer från andra artiklar tyder på att QSD modellen är den bästa att använda. Modellen ger bra data om oxidationsgraden men data från M1, M2 besättningen är inte fullt lika bra. Detta problem finns för vilken modell man än använder för biotit. En kort jämförelse med Mössbauer-spektrum av muskovit finns med i arbetet, muskovit är ett mineral som liknar biotit både kemiskt och strukturellt. Skillnaderna är dock stora i Mössbauer-spektrer, där muskovit ger bra data på M1, M2 besättningen medan biotit inte gör det. Anledningen till denna skillnad är troligtvis beroende på skillnaderna i kemisk uppbyggnad samt små skillnader i form av de två positionerna mellan de två mineralen.

Jonas Bermin, Department of Geology, Sub department of Mineralogy and Petrology, Sölvegatan 13, S-223 62 Lund, Sverige

1 Introduction

1.1 Origin of samples

This work is based on biotite samples originally described by Hainping et al. (1994). These samples have then been analysed using Mössbauer spectroscopy, a technique less familiar in the Dept of Mineralogy & Petrology, Lund University. A detailed explanation is therefore helpful. The explanation deals with the different Mössbauer hyperfine parameters, problems with interpretation of Mössbauer spectra and a brief theoretical background.

1.2 The problem with fitting Mössbauer spectra to biotite.

In Mössbauer spectroscopy of biotites it is easy to determine the oxidation state and coordination number of iron (Rancourt 1994a). The major difficulty is determining whether the octahedral Fe^{2+} is in trans- or cis configuration (M1 or M2). According to Rancourt (1994b) this is not possible to do. However, other work, such as Goodman and Wilson (1973) and Rice and Williams (1969) suggest that this can be done. Moreover, Ferrow (1987) observed well-resolved lines for Fe^{2+} in highly oxidised biotite ascribed to Fe^{2+} in cis and trans configurations. Keeping this problem in mind the approach to M1 and M2 site occupation in biotite using Mössbauer spectroscopy was studied carefully. The reason that it is hard to decide site occupation for iron in M1 and M2 is that the Mössbauer lines overlap, resulting in one asymmetrical broad line that is the sum of the two actual lines.

The difference between Fe^{2+} and Fe^{3+} is easier to decide as the different lines are clearly separated in the Mössbauer spectrum.

1.3 Aim of this study.

This study is made as a Masters thesis in geology with the aim of studying the dependence of pH on biotite and to find a good way to determine the occupancy of M1 and M2 positions in the octahedral sites using Mössbauer spectroscopy. The study also tries to find an answer to why the Mössbauer spectra of biotite and muscovite show big differences in the M1 and M2 positions.

2 Materials and experimental techniques

The biotites used in this study come from the collection of the mineralogical museum of the Institute of Earth Sciences, Uppsala University. They were treated as described in Hainping et al (1994). The samples were crushed into coarse pieces and then handpicked to get the purest samples. These samples were then ground to 63-124 μm. The mineralogical purity was checked with a diffractometer to be 95%. The chemical composition of the biotite was analysed by SGAB Analys (Luleå). The chemical formula is:

$K_{0,86}(Al_{0,10}Mg_{0,97}Ti_{0,12}Mn_{0,02}Fe_{1,80})(AL_{1,26}Si_{2,74})O_{10}(OH)_2$.

In the lab in Uppsala, small amounts of the biotite were put into bottles with a solution containing 5ppm Be with fixed pH. The bottles were shaken continuously at room temperature. Three different pH's were used, 2, 6 and 9. All of the bottles were prepared under the same conditions, but run for duration of 30 minutes to 20 days. Four minutes before the end of the set time the bottles were centrifuged to make

Time	Concentration (mmol/l)			
(minutes)	Si	Al	Fe	Mg
		In pH2 solution		
30	0.041	0.071	0.076	0.018
60	0.10	0.073	0.088	0.021
1440	0.24	0.25	0.33	0.054
4320	0.46	0.45	0.59	0.14
14400	1.07	0.87	0.97	0.25
28800	1.46	1.12	1.04	0.28
		In pH6 solution		
30	0.066	0.013	<0.0001	0.003
4320	0.050	0.009	<0.0001	0.004
14400	0.014	0.012	0.0007	0.004
		In pH9 solution		
30	0.029	0.20	0.0003	0.003
4320	0.005	0.39	0.0009	0.003
14400	0.061	0.39	0.0001	0.003

Table 1. The results from the experiments made by Hainping et al. (1994) for the different pHs.

the solid particles sink to the bottom of the bottle. After centrifugation the solution was used for determining the concentration of a number of elements (Table 1). The solid particles were dried at room temperature and it is these samples that have been used in this study.

Mössbauer spectra were recorded at room temperature on a Mössbauer spectrometer with a ^{57}Co/Rh source. A simple spectrometer interfaced to a PC computer is used for collecting the data (Mashlan *et al.*, 1994). The PC controls the form and amplitude of the velocity signal, the energy window of the single-channel analyser and the high voltage of the scintillation $YAlO_3$: Ce (YAP) crystal detector. Mössbauer spectra in lengths of 1024 channels were accumulated using constant acceleration mode. Velocities were calibrated using Fe-foil with a thickness of 25 μm supplied by Dupont Pharma.

Thin tablets were prepared by mixing the sample with a transoptic material, called lucite, until the weight was about 150 mg. The mix were then put into a steel cylinder and quickly heated to about 140 degrees Celsius. The warm cylinder was now pressed from top and bottom and allowed to cool off to room temperature like this. After carefully opening the cylinder, the tablet measuring 10 mm in diameter and less than 2 mm thick, could be extracted and put in a plastic bag waiting for analyse. This procedure was worked out by Annersten (1974). Since sheet silicates have preferred orientation, the tablets were put into the spectrometer at an angle of 54.7° to obtain as symmetric absorption doublets as possible. The spectra were computer-fitted using the Voigt-based quadrupole splitting distributions, QSD,

program in Recoil, a commercially available Mössbauer spectral analysis software package.

3 Mössbauer Spectroscopy

3.1 Theoretical background

Ever since Rudolf Mössbauer discovered that atomic nuclei absorb and emit gamma rays without loss of energy, also known as recoil free resonance, in 1957, the method has been used as an important tool in mineralogical research. His discovery is called the Mössbauer effect and gave him the Nobel Prize in physics in 1963. The effect is used in Mössbauer spectroscopy by putting a sample in between a gamma ray emitter and an absorber. The emitter has to emit photons of the correct energy levels to excite the sample. In this case the atom used both as source and sample is ^{57}Fe. To make the source emit photons of the correct type ^{57}Co decays to an excited, non-stable, state of ^{57}Fe. This reaction can be written: $^{57}Co_{27} + {}^{0}\beta_{1} \rightarrow {}^{57}Fe_{26}$. As the produced Fe falls to its ground state it will emit three different gamma rays. These gamma rays are of the energies 14.4, 123 and 137 keV. In Mössbauer spectroscopy the 14.4 keV gamma ray is used (figure 1). The reason that the 14.4 keV gamma ray is best to use is that the probability of recoil free absorption/emitting is higher with a low energy gamma ray.

In order to get information out from the study it is interesting to alter the energy of the gamma ray slightly. This is easily done by putting the source on a loudspeaker film. By vibrating the film back and forth with the speed of a few mm/s the energy of the emitted gamma rays will be altered slightly because of the Doppler effect. An example of an experimental set-up is shown in figure 2. A radioactive source is mounted onto a drive system.
One measures as a function of velocity either the count rate of the transmitted radiation through the sample or the count rate of the backscattered electrons, x-rays or gamma quanta. In the former, one obtains information on the bulk while in the latter the information

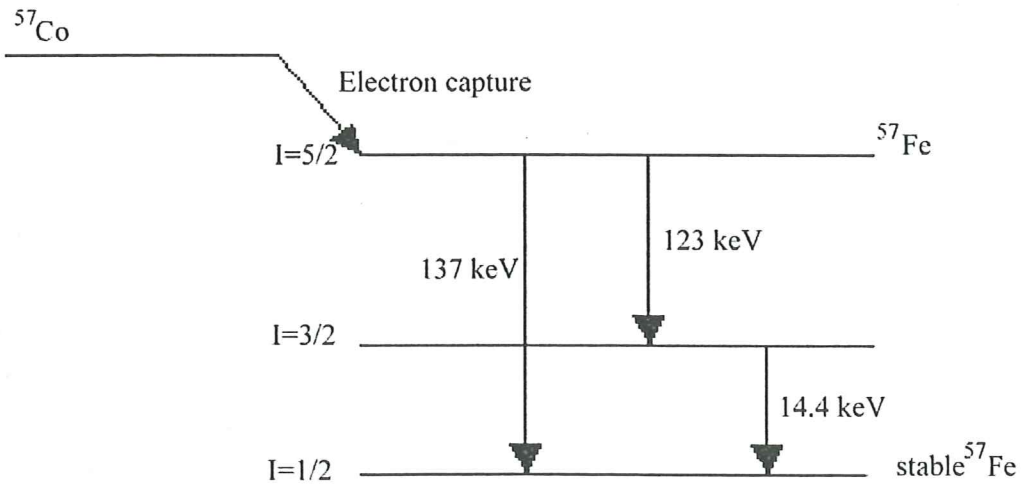

Fig 1. Energy diagram describing the energy levels of the different states of ^{57}Fe.

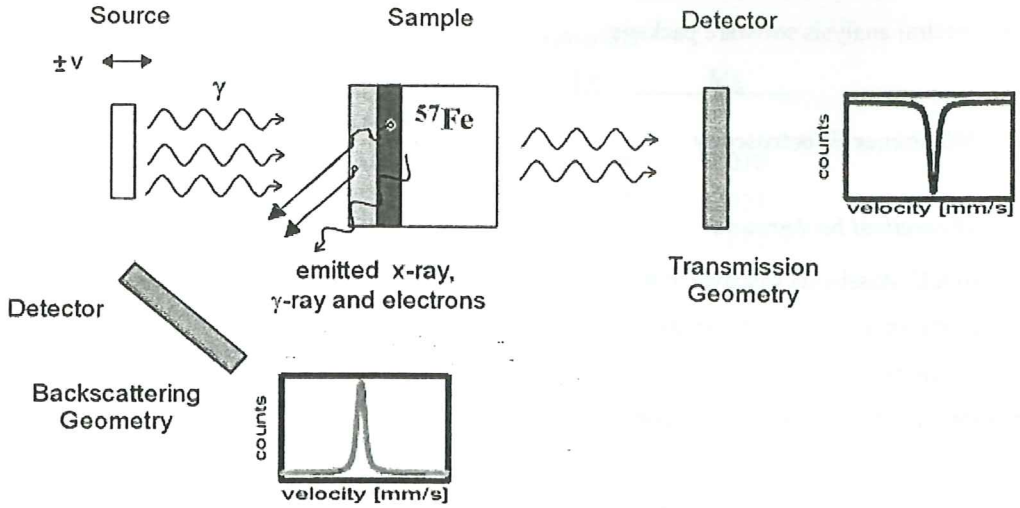

Figure 2. Schematic set-up of a Mössbauer spectrometer.

gathered comes from the first 200-300 nm of the sample, providing information on the surface chemistry.

3.2 Isomer shift

The isomer shift is a parameter in Mössbauer spectroscopy that describes the electrostatic interaction between the nucleus and the electrons. When this interaction changes there will be a slight change in the energy needed to excite the nucleus, this will lead to a shift in the spectrum. An example is the difference between Fe^{2+} and Fe^{3+}. These two ions have different numbers of electrons but the same number of protons and will therefore have a major difference in the interaction between the nucleus and the electrons surrounding it. The Isomer shift will increase with the number of electrons around the nucleus. This means that the Fe^{3+} will have a smaller Isomer shift than the Fe^{2+}. If the ground state and the excited state would react in the same way to this electrostatic interaction they would both have energy levels that would differ with the same amount and the resulting energy leap would always be the same. Fortunately for Mössbauer spectroscopy, the ground state and the excited state will not act in the same way and therefore the energy needed to excite the nucleus will differ.

3.3 Quadrupole splitting

When the nucleus goes from its ground state to the excited state because of the 14.4 keV photon the quantum number I changes from $I = 1/2$ to $I = 3/2$. This means that the quantum number m_I can have four different values as $m_I = I, I\text{-}1, \ldots, -I$. The ground state will only have one energy level given that there is no magnetic field present. However, the excited states have two different energy levels ($m_I = \pm 3/2$ *and* $m_I = \pm 1/2$), which will produce two separate absorption levels. This separation or split in energy levels is associated with the electrons of the surrounding ligands and it is called the Quadrupole split. The Quadrupole split is therefore useful to determine the coordination number of the Fe siteA way to describe what actually happens in the nucleus is to imagine the nucleus as a slightly elongated

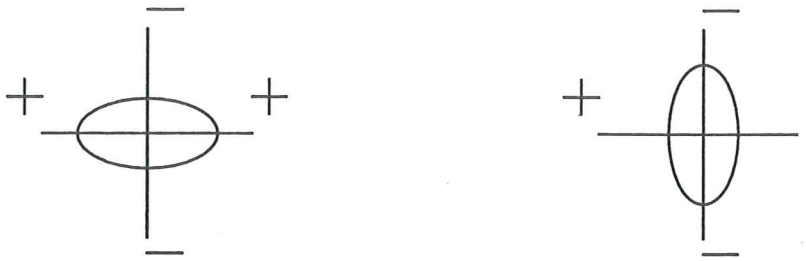

3a 3b

Fig 3. The difference between the quanta symbolises a change in the shape of the nucleus. This change produces differences in energy.

sphere. If the sphere is elongated in different directions there will be different energy levels depending on the environment near the atom. In figure 3 there is a difference between 3a and 3b. 3a has a higher energy than 3b as the nucleus is of positive charge. The reason why there is no difference is the energy levels for the ground state might be that the nucleus doesn't act like an elongated sphere for its quantum number (I = 1/2). It might instead be a circular sphere and because of that it can't have different directions.

3.4 Magnetic hyperfine splitting

If the sample are analysed while being in a magnetic field, or if they are magnetic on their own the Mössbauer spectra will look completely different from what has been described so far. The difference is that now

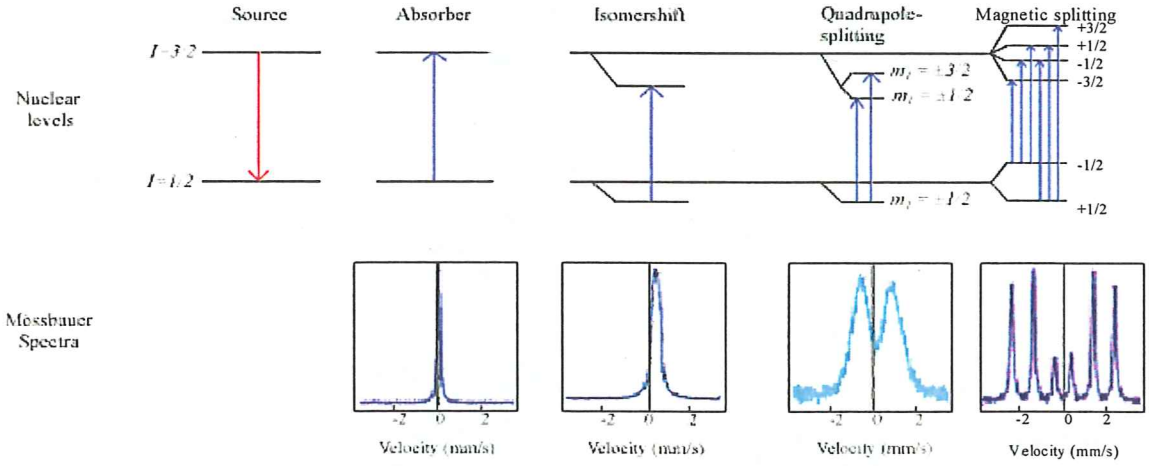

Figure 4. This figure shows the different Mössbauer spectra described in the text. First there is a single line that is centred in the spectrum. This is what happens when the absorber is a single nucleus without any surrounding electrons or atoms. The second spectrum, the isomer shift, is also a single line but it is not centred. This will be the case for an atom that is situated within a crystal where all atoms are the same and all distances between atoms are equal. The third spectrum, the quadrupole spectrum, shows what happens if the sample is in a crystal where the surrounding atoms are not the same in all directions. The last spectrum shows the magnetic split that will be produced if the sample is magnetic or put in a magnetic field.

there will be six lines instead of the double lines produced by the quadrupole splitting. The reason is that the different magnetic spins will change in energy depending on the magnetic field. The ground state will have two energy levels and the excited state will have four. These different energy levels should be able to produce eight lines if all was working ideally. There are however only six possible lines, this has to do with not permitted quantum leaps.

4 Modelling quadrupole splitting

4.1 cis vs trans configurations

The difference between the M1 and M2 positions in a biotite was studied using a computer program called Atoms. In this program one can measure the angles and distances within the biotite structure. The two positions differ in the way that they connect with the surrounding ligands. Both positions are in the shape of octahedrons, which means that they have a central cat ion surrounded by six anions. The central cat ions are surrounded by four oxygen anions and two hydroxyl groups. The difference is that in the M1 the OH groups have a trans configuration while in the M2 the OH groups have cis configuration. The cis means that two OH groups are connected next to each other in the structure while the trans means that the OH groups connect opposite to each other. Figure 5 shows the structure of the biotite. Because of the

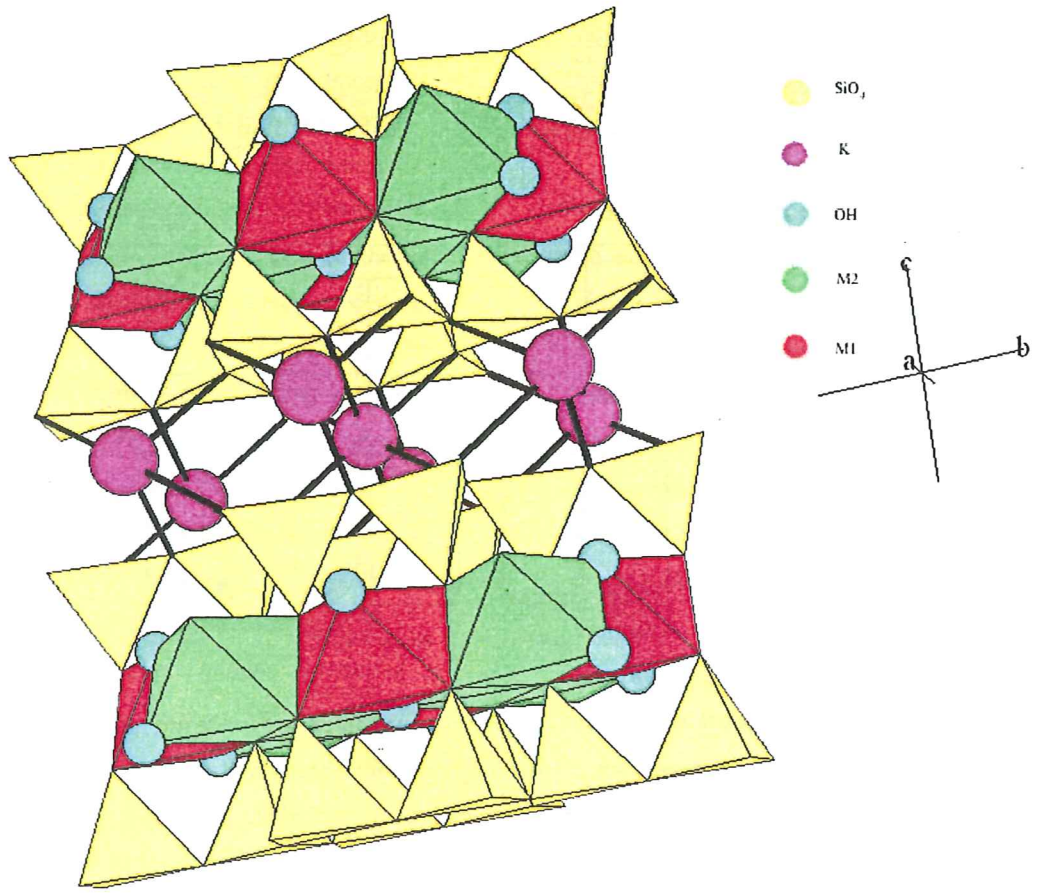

Figure 5. The atomic structure of a biotite. The trans positions, or M1 are the green octahedrons and the cis positions, or M2, are the red octahedrons.

symmetry of the structure there is twice as many M2 than M1 positions.

4.2 Octahedral site distortion

The distances between the central atom and the surrounding atoms for the octahedral positions M1 and M2, for biotite were measured using Atoms. The biotite used is described by Hazen and Burnham (1973) and the structural parameters are presented in Table 3 together with the structural parameters of muscovite as described by Lin and Bailey (1984). If the positions would have been symmetrical, all six metal-oxygen (M-O) distances should be identical and the angles between oxygen-metal-oxygen (O-M-O) should all be 90 degrees. As seen in Table 3 this is not the case. There are two different forms of distortion of the octahedral site. The first case deals with the difference in distance between the metal and the oxygens and the second case deals with the distortion of the angles between the O-M-O. The first distortion can be measured in many ways. In this study the method defined by Brown & Shannon (1973) will be used where they defined a distortion parameter:

$$\Delta_0 = \frac{1}{6}\sum\left|\frac{l_i - l_m}{l_m}\right|, \qquad (1)$$

where l_i is the measured O-M distance and l_m is the average M-O distance of the octahedron. This summation is made over all of the six O-M distances.

For the second type of distortion, the distortion defined by Robinson et al. (1971) was used. They defined an angular distortion parameter:

$$\sigma_0 = \frac{1}{11}\sum\left|(\Theta_1 - 90)^2\right|, \qquad (2)$$

where Θ_i is the measured O-M-O angle. The summation is made over the twelve O-M-O angles.

The two different parameters Δ_0 and σ_0 are difficult to selectively correlate to the observed Mössbauer spectra. The correct approach is to combine the two distortion parameters as one. However, this will cause a problem, as the first parameter doesn't have a unit while the second one does. To avoid the problem it is possible to redefine the parameter σ_0 as:

$$\sigma_0 = \frac{1}{11}\sum\left|\frac{\Theta_i - 90}{90}\right| \qquad (3)$$

By doing this we remove the unit from the second parameter as well and it is then easy to combine them to a new distortion parameter:

$$\Omega = \Delta_0 + \sigma_0 \qquad (4)$$

The different distortion parameters obtained for biotite and muscovite using the data of Hazen and Burnham (1973) and Lin and Bailey (1984) are listed in Table 2.

It is clearly shown that the M2 position in muscovite is strongly distorted if it is compared with the three other positions in Table 2. This difference in distortion could be the reason

why the overlap of the two doublets originating from the M1 and M2 positions in the Mössbauer spectrum of muscovite is less severe than in biotite.

5 Results

5.1 Fitting methods

Two different approaches to fitting the spectra were compared. First the widespread method using Lorentzian doublets and then a method called Quadrupole splitting distribution (QSD). These two different methods were tested on the sample with the best statistical result (jb375). The different models were applied with the same number of free parameters and then the values of the reduced χ^2 were compared. The resulting Mössbauer spectra are shown in figure 6 and the Mössbauer parameters are listed in Table 3. To get the same number of free parameters, two of the three widths of the QSDs were set as free parameters (Rancourt 1994a).

As Table 3 shows, for the same number of free parameters, the QSD model gives a better fit than the Lorentzian fit model. As Rancourt (1994a) demonstrated the QSD is also easier to correlate with the real physical positions. Due to the results from this comparison ($\chi^2_{red} = 0.89$ versus 1.5) the rest of the samples were all fitted using QSDs.

	Paragonite (Muscovite)				Phlogopite (Biotite)			
	M1		M2		M1		M2	
	O-M	O-M-O	O-M	O-M-O	O-M	O-M-O	O-M	O-M-O
	1.908	92.2	2.253	81.1	2.071	85.8	2.080	85.3
	1.923	92.3	2.253	81.1	2.071	85.6	2.080	94.7
	1.907	92.5	2.249	79.6	2.083	95.2	2.080	96.5
	1.930	94.8	2.249	79.6	2.083	96.5	2.080	83.5
	1.891	92.5	2.160	79.6	2.040	95.2	2.030	94.7
	1.891	94.8	2.160	79.6	2.040	85.6	2.030	83.5
		78.8		98.9		96.5		96.5
		78.6		98.9		83.2		85.3
		77.0		100.4		96.0		83.5
		98.9		100.4		96.0		96.5
		96.1		100.4		83.2		96.5
		96.1		100.4		81.2		83.5
Average	1.908	90.38	2.221	90.00	2.065	90.00	2.063	90.00
Δ_0	0.006		0.018		0.008		0.011	
σ_0	0.070		0.110		0.066		0.065	
Ω	0.076		0.128		0.074		0.076	

Table 2. O-M is the distance in Å between the central metal atom and the ligand oxygen in the octahedral site, O-M-O is the angle between two oxygen and the central metal atom in the polyhedron. The different distortion parameters are listed at the bottom of the table.

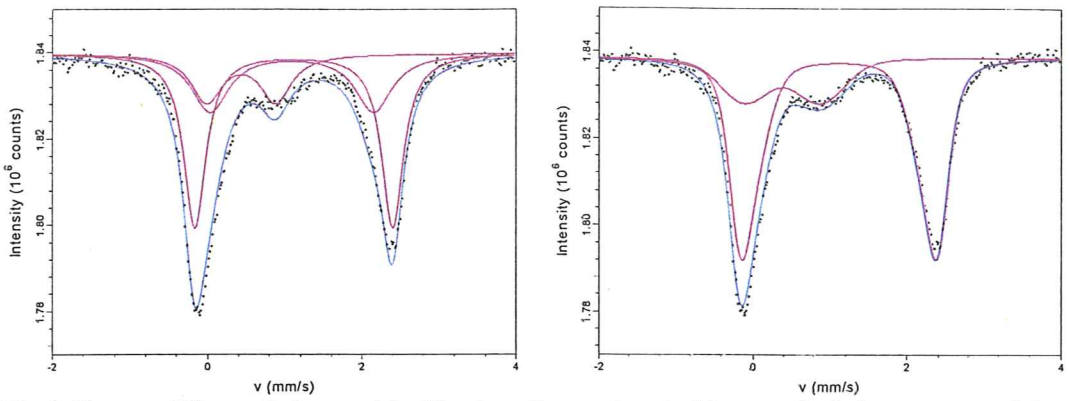

Fig 6. The two different fitting models. The three Lorentzian doublets are the left spectrum and the QSD is the right one.

Fit	Site	δ (mm/s)	Δ (mm/s)	σ (mm/s)	Area (%)	BG (MC/ch)	No. par.	χ^2_{red}
3 Lorentzian	[3+]	0.441	0.896	0.242	19.70			
	[2+]-1	1.12	2.563*	0.172*	51.30			
	[2+]-2	1.09	2.12*	0.29*	29.00	1.840	9	1.5
QSD	[3+]	0.39	0.981	0.565	25.43			
	[2+]-1	1.13	2.563*	0.200	48.58			
	[2+]-2	1.13*	2.12*	0.29*	25.99	1.838	9	0.89

*Table 3. Fitting parameters for 3 Lorentzians and 3 QSDs on the same sample. * indicates values that were frozen during the fit, δ = Isomer shift, Δ = Quadrupole split, σ = width of line at half depth, BG = Back ground.*

5.2 Experimental results

The different samples were named in the order they were analysed. The order was made without any special meaning except to try and fit in as many samples as possible during the time (this means that the samples with low mass often were left in the spectrometer during the weekends).

5.3 pH6 experimental results

The spectra were all treated as described before. Figure 7 shows some representative spectra recorded and fitted from the experiments with pH6. The Mössbauer parameters obtained are listed in Table 4.

It is easy to see from Table 4 that, at pH 6, the amount of Fe^{3+} in the spectra's increases with treatment time, though the increase is small. The Table also shows that there is a visible change in the M1/M2 ratio within the series. Though the change is not regular, Table 4 shows that the percentage of iron in M1 increases with time while that in M2 decreases, indicating that the rate of oxidation in M2 is faster than in M1.

5.4 pH2 experimental results

Similarly representative spectra for the pH2 experimental series are shown in figure 8 and

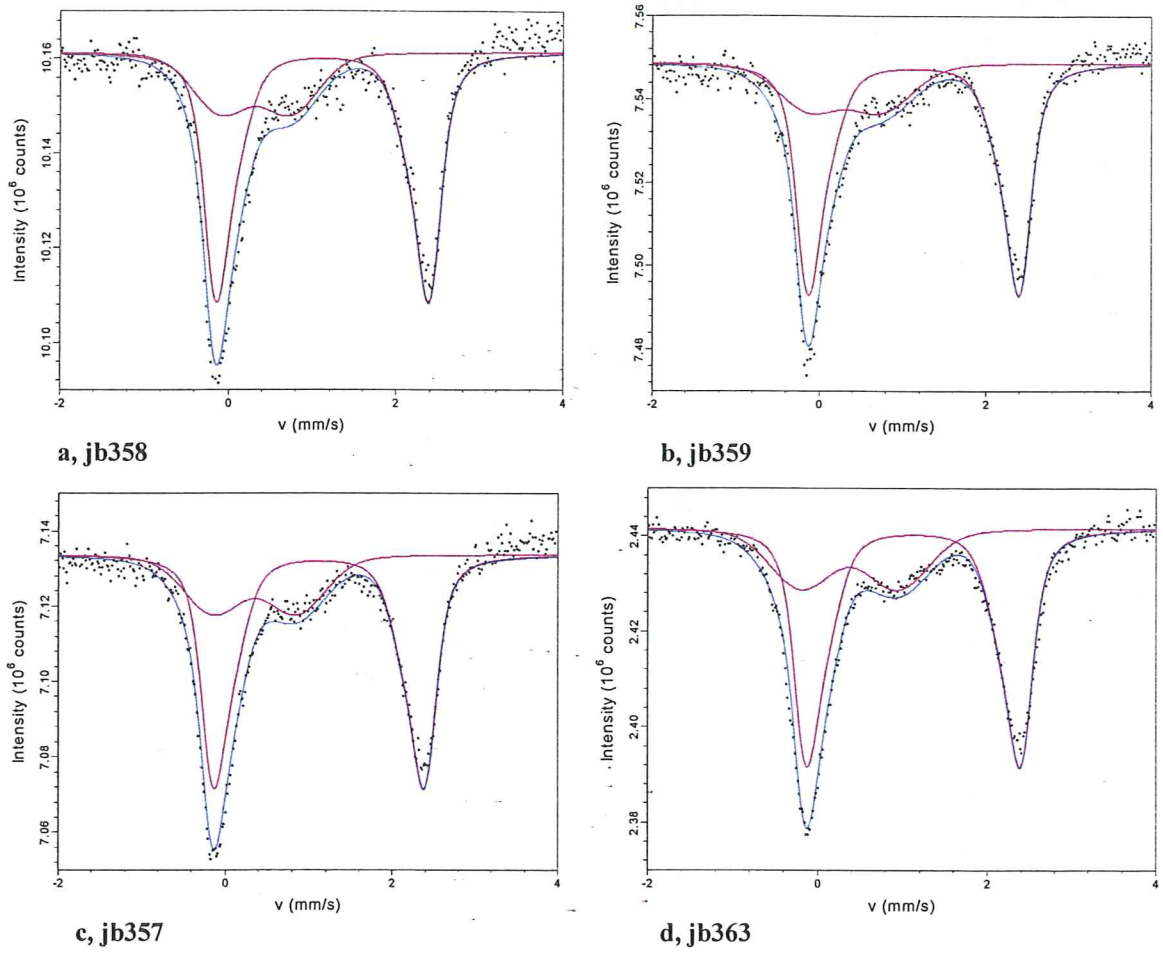

Figure 7. This figure shows different spectra's from the pH6 experiments. These are all fitted, as described in the text, with the quadrupole splitting distribution method. There are two visible doublets in every spectrum, the deeper of them derives from Fe^{2+} and the second one, with smaller quadrupole split and smaller isomer shift is the Fe^{3+} doublet. The spectra are sorted after how long they were in the solution. a was in the solution for a shorter time than b and so on.

Time (minutes)	Fe^{2+}(%)	M1 (%)	M2 (%)	Fe^{3+}(%)	Sample name
		In pH6 solution			
30	71.7	32.7	67.3	28.3	jb358
60	73.7	32.6	67.4	26.3	jb362
480	70.2	36.5	63.5	29.8	jb360
1440	71.7	30.8	69.2	28.3	jb361
4320	72.5	32.3	67.7	27.5	jb364
7200	73.1	31.6	68.4	26.9	jb359
14400	70.6	38.1	61.9	29.4	jb357
28800	69.4	39.0	61.0	30.6	jb363

Table 4. The different positions from the pH6 experiments presented in percent.

the corresponding parameters are listed in Table 5. Once again it is obvious that the Fe^{3+} increases with the time in the pH2 series as well. The M1/M2 ratio also changes, again increasing in M1 and decreasing in M2.

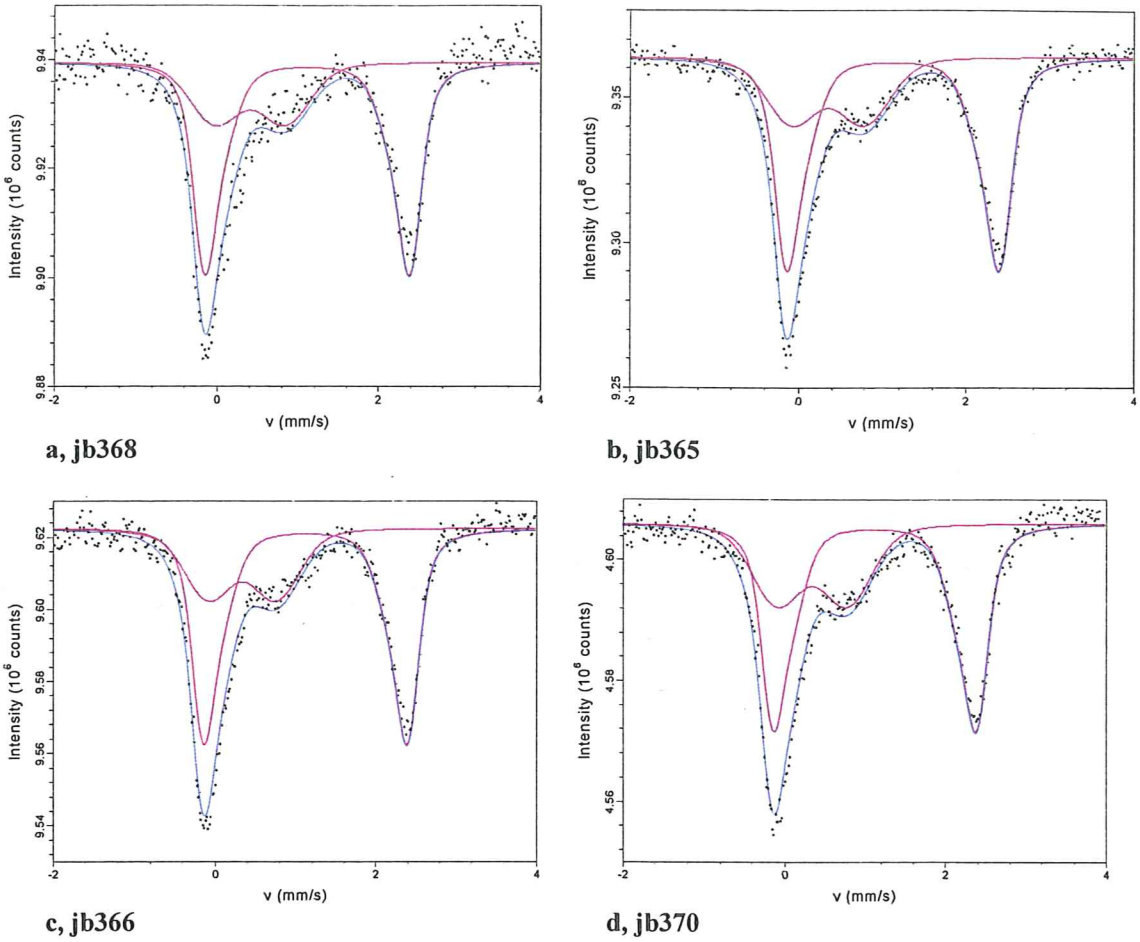

Figure 8. This figure shows different spectra's from the pH2 experiments. The spectra are sorted after how long they were in the solution. a was in the solution for a shorter time than b and so on.

5.5 pH9 experimental results

Finally, representative spectra for the pH9 series are shown in figure 9 and the relative intensities for the Fe sites are given in Table 6. Here, however, it is not very easy to see any clear trends in changes in the amount of Fe3+ and in the M1/M2 ratio. This might be due to the difference in duration time. In pHs 2 and 6 the samples were kept in the solution for twice as long as for those in pH 9. There is however a vague trend that the Fe^{3+} increases at the end.

Time (minutes)	Fe^{2+}(%)	M1(%)	M2(%)	Fe^{3+}(%)	Sample name
		In pH2 solution			
30	68.7	29.7	70.3	31.3	jb368
60	67.5	32.2	67.8	32.5	jb365
480	67.3	32.1	67.9	32.7	jb366
4320	69.1	39.3	60.7	30.9	jb369
28800	63.3	39.0	61.0	36.7	jb370

Table 5. Site occupation for the pH2 experiments presented in percent.

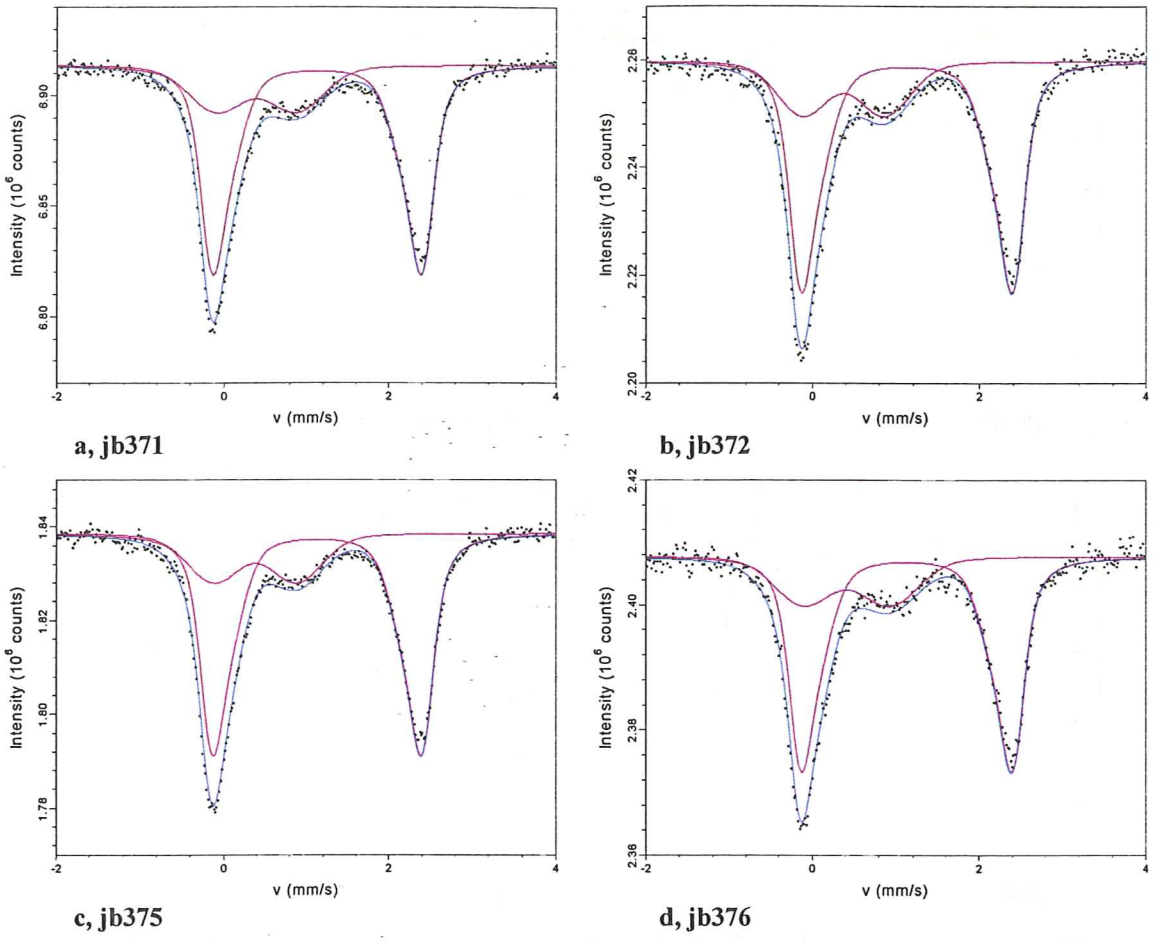

Figure 9. This figure shows different spectra's from the pH9 experiments. The spectra are sorted after how long they were in the solution. a was in the solution for a shorter time than b and so on.

Time (minutes)	Fe^{2+}	M1(%)	M2(%)	Fe^{3+}	Sample name
		In pH9 solution			
30	73.5	34.9	65.1	26.5	jb371
1440	74.4	31.7	68.3	25.6	jb373
4320	73.9	35.8	64.2	26.1	jb372
7200	74.7	36.4	63.6	25.3	jb375
14400	72.8	36.6	63.4	27.2	jb376

Table 6. The different positions from the pH9 experiments presented in percent.

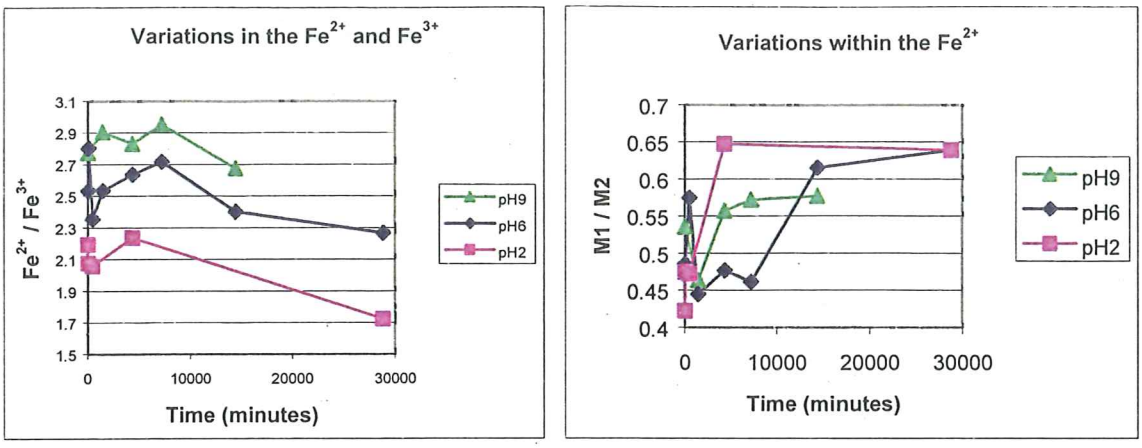

Figure 10. This figure shows the relation between Fe^{2+} and Fe^{3+} over time for the three different pHs.

The results from the three different pH experiments are summarised in figure 10.

6 Discussion and conclusion

From the interpretation of the spectra it seems clear that Fe^{3+} increases with time for all three pH series (see figure 10). It is also easy to see that the oxidation has been stronger in the more acidic experiments. Unfortunately in this study, data from the original, unaltered, biotite sample is not available. This is obvious in Fig. 10 where the three different lines start at different Fe^{2+}/Fe3+ ratios, since the Mössbauer data available is for samples that have been treated for at least 30 minutes.

To show what happened after these first 30 minutes two new plots were made. These new plots were made with the average of the three 30-minute values as a reference value. The remaining data points of the three series were recalculated to account for the averaging done for the 30 minutes runs. If the difference between the 30 minutes run and the average value is positive for a given series, then the value of the remaining runs within that series is reduced by the same amount and vice versa. The results after recalculation are plotted for both the Fe^{2+}/Fe^{3+} ratio and the M1/M2 ratio in figure 11.

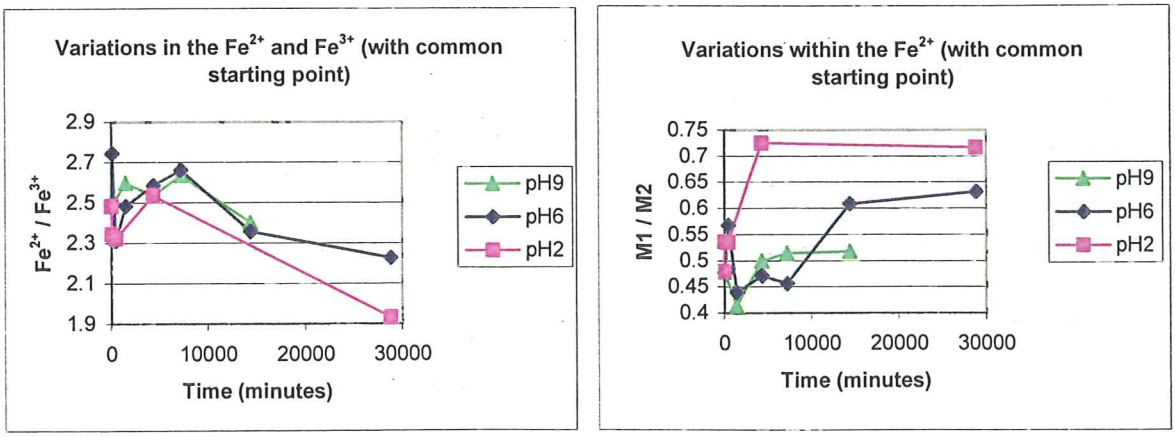

Figure 11. Plots showing the same as in Figure 10 with common starting points.

In the new plot, the Fe^{2+}/Fe^{3+} ratio for the three series approaches each other. It is easy to see that the difference in the oxidation ratio is now less. This means that the large differences shown in Fig. 10 were due to the differences already built up during the first 30 minutes. The plot showing the M1/M2 relation doesn't show the same pattern. The reason to this might be that the two sites keep on changing after the first 30 minutes in a greater way than the Fe^{2+}/Fe^{3+}.

All the results show that the biotites that had been treated at lower pH are more altered than the biotites treated at higher pH. This is visible both in the original diagrams and in the new diagrams with common starting point.

The model used for interpreting the Fe^{2+}/Fe^{3+} ratio seems to be accurate as the plots in figures 10 and 11 show some kind of evolution with time. If the results had shown random evolution the model would most likely be wrong. However, the evolution in the M1/M2 ratio is not fully random though the correlation is not perfect either, suggesting that the model used may not be sufficient to describe site population in M1 and M2.

The distortion in the M1 and M2 positions of biotite and muscovite seems to be the main reason to why the two minerals show big differences in the Mössbauer spectra. The distortion of the M1 and M2 sites in biotite appears to be similar while the distortion of the muscovite shows larger difference between the two sites. The difference in the degree of distortion between biotite and muscovite together with the chemical difference of the octahedral sites (Al is the main cat ion in muscovite while in biotite Mg, Fe and Al are present) may be the reason for the difference in Mössbauer spectra between the two.

7 Acknowledgements

I am very grateful for all the advice and assistance from my supervisor Dr. Embaie A. Ferrow. I would also like to thank Professor Anders Lindh for always taking the time to answer any questions.

8 References

Annersten H. (1974) Mössbauer Studies of Natural Biotites. American Mineralogist, Volume 59:143-151

Brown ID., Shannon RD. (1972) Empirical bond strength-bond length curves for oxides. Acta Crystallographica. Section A. Crystal Physics, Diffraction, Theoretical and General Crystallography. 28:107

Ferrow E. (1987) Mössbauer and x-ray studies on the oxidation of annite and ferriannite. Phys. Chem. Minerals, 14:270-275

Goodman B.A. and Wilson M.J. (1973) A study of the weathering of a biotite using the Mössbauer effect. Mineralogical Magazine, vol. 39:448-54

Hainping Ye, Aldahan A.A. and Possnert G. (1994) Beryllium distribution between minerals and solution: laboratory experiments and applicat ion to the distribution of Beryllium-10 in continental sediments.

Hazen and Burnham (1973) Phlogopite. American Mineralogist, Volume 58:889

Lin Cheng-Yi and Bailey S.W. (1984) The crystal structure of paragonite-$2M_1$. American Mineralogist, Volume 69:122-127

Mashlan M., Zak D., Cholmeckij A., Evdokimov V., Misevic O., Fedorov A., Lopatik A., Snasel V. (1994) The PC-AT based Mössbauer spectrometer. Acta Universitaris Palackinae Olomoucensis. Facultas Rerum Naturalium, Physica XXXIII, 116.

Rancourt D.G. (1994a) Inadequacy of Lorentzian-line Doublets in Fitting Spectra Arising from Quadrupole Splitting Distributions. Phys Chem Minerals 21:244-249

Rancourt D.G. (1994b) Problem of Resolving cis and trans Octahedral Fe^{2+} Sites. Phys Chem Minerals 21:250-257

Rice C.M. and Williams J.M. (1969) A Mössbauer study of biotite weathering. Mineralogical Magazine, vol. 37, NO. 286

Robinson K., Gibbs GV., Ribbe PH. (1971) Quadratic elongation: a quantitative measure of distortion in coordination polyhedra. Science 172:567-570

Tidigare skrifter i serien "Examensarbeten i Geologi vid Lunds Universitet":

74. Rees, Jan, 1996: A new hybodont shark fauna from the Upper Jurassic Vitabäck Clays at Eriksdal, Scania, southern Sweden.
75. Bengtsson, Fredrik, 1996: Paleomagnetisk undersökning av senpaleozoiska gångbergarter i Skåne; Kongadiabas, melafyr och kullait.
76. Björngreen, Maria, 1996: Kontrollprogram vid avfallsupplag - en utvärdering.
77. Hansson, Anders, 1996: Adaptations and evolution in terrestrial carnivores.
78. Book, Jenny, 1996: A Light Microscopy and Scanning Electron Microscopy study of coccoliths from two bore holes along the City Tunnel Line in Malmö, Sweden.
79. Broström, Anna, 1996: The openess of the present-day landscape reflected in pollen assem-blages from surface sediments in lakes - a first step towards a quantitative approach for the reconstruction of ancient cultural landscapes in south Sweden.
80. Paulsson, Oskar, 1996: Sevekomplexets utbredning i norra Kebnekaise, Skandinaviska Kaledoniderna.
81. Sandelin, Stefan, 1997: Tektonostratigrafi och protoliter i Mårma-Vistasområdet, Kebnekaise, Skandinaviska Kaledoniderna.
82. Meyerson, Jacob, 1997: Uppermost Lower Cambrian - Middle Cambrian stratigraphy and sedimentary petrography of the Almbacken drill-core, Scania, southern Sweden.
83. Åkesson, Mats, 1997: Moränsedimentologisk undersökning och bestämning av postglacialt bildade järn- och manganmineral i en drumlinformad rygg.
84. Ahlgren, Charlotte, 1997: Late Ordovician communities from North America.
85. Strömberg, Caroline, 1997: The conodont genus *Ctenognathodus* in the Silurian of Gotland, Sweden.
86. Borgenlöv, Camilla, 1997: Vätskeinklusioner som ledtrådar till bildningsmiljön för Bölets manganmalm, Västergötland, södra Sverige.
87. Mårtensson, Thomas, 1997: En petrografisk och geokemisk undersökning av inneslutningar i Nordingrågraniten.
88. Gunnemyr, Lisa, 1997: Spårämnesförsök i konstgjort infiltrerat vatten - en geologisk och hydrogeologisk studie av Strömsholmsåsen, Hallstahammar, Västmanland.
89. Antonsson, Christina, 1997: Inventering, hydrologisk klassificering samt bedömning av hydrogeologisk påverkan av våtmarksområden i samband med järnvägs-tunnelbyggnation genom Hallandsåsen, NV Skåne.
90. Nordborg, Fredrik, 1997: Granens markpåverkan - en studie av markkemi, jordmånsbildning och lermineralogi i gran- och lövskogsbestånd i södra Småland.
91. Dobos, Felicia, 1997: Pollen-stratigraphic position of the last Baltic Ice Lake drainage.
92. Nilsson, Johan, 1997: The Brennvinsfjorden Group of southern Botniahalvøya, Nordaustlandet, Svalbard - structure, stratigraphy and depositional environment.
93. Tagesson, Esbjörn, 1998: Hydrogeologisk studie av grundvattnets kloridhalter på östra Listerlandet, Blekinge.
94. Eriksson, Saskia, 1998: Morängenetiska undersökningar i klintar vid Greifswalder Boddens södra kust, NÖ Tyskland.
95. Lindgren, Johan, 1998: Early Campanian mosasaurs (Reptilia; Mosasauridae) from the Kristianstad Basin, southern Sweden.
96. Ahnesjö, Jonas, B., 1998: Lower Ordovician conodonts from Köpings klint, central Öland, and the feeding apparatuses of *Oistodus lanceolatus* Pander and *Acodus deltatus* Lindström.
97. Rehnström, Emma, 1998: Tectonic stratigraphy and structural geology of the Ålkatj-Tielma massif, northern Swedish Caledonides.
98. Modin, Anna-Karin, 1998: Distributionen av kadmium i moränmark kring St. Olof, SÖ Skåne.
99. Stockfors, Martin, 1998: High-resolution methods for study of carbonate rock: a tool for correlating the sedimentary record.
100. Zillén, Lovisa, 1998: Late Holocene dune activity at Sandhammaren, southern Sweden -chronology and the role of climate, vegetation, and human impact.
101. Bernhard, Maria, 1998: En paleo-ekologisk-paleohydrologisk undersökning av våtmarkskomplexet Rolands hav, Blekinge.
102. Carlemalm,Gunnar, 1999: En glacialgeologisk studie av morän och moränfyllda sprickor i underliggande sandursediment, Örsjö, Skåne.
103. Blomstrand, Malou, 1999: 1992-1998 Seismicity and Deformation at Mt.Eyjafjallajökull volcano,South Iceland.
104. Dahlqvist, Peter, 1999: A Lower Silurian (Llandoverian) halysitid fauna from the Berge Limestone Formation, Norderön, Jämtland, central Sweden.
105. Svensson, Magnus A., 1999:Phosphatized echinoderm remains from upper Lower Ordovician strata of northern Öland, Sweden - preservation, taxonomy and evolution.
106. Bengtsson, Anders, 1999: Trilobites and bradoriid arthropods from the Middle and Upper

Cambrian at Gudhem in Västergötland, Sweden.

107. Persson, Christian, 1999: Silurian graptolites from Bohemia, Czech Republic.
108. Jacobson, Mattias, 1999: Five new cephalopod species from the Silurian of Gotland.
109. Augustsson, Carita, 1999: Lapillituff som bevis för underjurassisk vulkanism av strombolikaraktär i Skåne.
110. Jensen, Sigfinn J., 1999: En silurisk transgressiv karbonatlagerföljd vid S:t Olofsholms stenbrott, Gotland.
111. Lund, Mats G., 1999: En strukturgeologisk modell för berggrunden i Sarves-vagge - Luottalako-området, Sareks Nationalpark, Lappland.
112. Magnusson, Jakob, 1999: Exploration of submarine fans along the Coffee Soil Fault in the Danish Central Graben.
113. Wickström, Jenny, 1999: Conodont biostratigraphy in Volkhovian sediments from the Mäekalda section, north-central Estonia.
114. Sjögren, Per, 1999: Utmarkens vegetationsutveckling vid Ire i Blekinge, från forntid till nutid - en pollenanalytisk studie.
115. Sälgeback, Jenny, 1999: Trace fossils from the Permian of western Dronning Maud Land, Antarctica.
116. Söderlund, Pia, 1999: Från gabbro till granatamfibolit. En studie av metamorfos i Åkermetabasiten väster om Protoginzonen, Småland.
117. Jönsson, Karl-Magnus, 2000: Sedimentologiska och litostratigrafiska undersökningar i södra Malmös kvartära avlagringar, södra Sverige.
118. Romberg, Ewa, 2000: En sediment- och biostratigrafisk undersökning av den tidigare Littorina-lagunen vid Barsebäck, SV Skåne, med beskrivning av en Preboreal klimatoscillation.
119. Bergman, Jonas, 2000: Skogshistoria i Söderåsens nationalpark. En pollenanalytisk studie i Söderåsens nationalpark, Skåne.
120. Lindahl, Anna, 2000: En paleoekologisk och paleohydrologisk studie av fuktängar i Bräkneåns dalgång, Bräkne-Hoby, Blekinge.
121. Eneroth, Erik, 2000: En paleomagnetisk detaljstudie av Sarekgångsvärmen.
122. Terfelt, Fredrik, 2000: Upper Cambrian trilobite faunas and biostratigraphy at Kakeled on Kinnekulle, Västergötland, Sweden.
123. Sundberg, Sven Birger, 2000: Vattenrening genom komplexbildning mellan järn och humusämnen - en litteraturstudie med försök
124. Sundberg, Sven Birger, 2000: Sedimentationsprocesser och avlagringsmiljö för en kantrygg kring platåleran vid Rydsgårds gods i backlandskapet söder om Romeleåsen, Skåne
125. Kjöllerström, Anders, 2000: En geokemisk studie av bergartsvariationen på Bullberget i västra Dalarna.
126. Cinthio, Kajsa, 2000: Senglacial och tidigholocen etablering och expansion av lövträd på en lokal i nordvästra Rumänien.
127. Lamme, Sara, 2000: Klimat- och miljöförändringar under holocen i Sylarnaområdet, södra svenska Skanderna, baserat på analys av makrofossil och klyvöppningar.
128. Jönsson, Charlotte, 2000: Geologisk och hydrogeologisk modellering av området mellan Bjuv och Söderåsen, nordvästra Skåne.
129. Kleman, Johan, 2001: Utvärdering av den underkambriska litostratigrafin på Österlen, södra Sverige.
130. Sundler, Malin, 2001: En jämförande studie mellan uppmätt och MACRO-simulerad pesticidutlakning på ett odlingsfält i Skåne.
131. Grönholm, Anna, 2001: Högtrycksmetabasiter i den södra delen av Mylonitzonen: fältgeologi, petrografi och metamorf utveckling.
132. Ekdahl, Magnus, 2001: En studie av Källsjögranitens deformationsmönster och kinematiska indikatorer inom Ullaredszonen.
133. Axheimer, Niklas, 2001: Middle Cambrian trilobites and biostratigraphy of the Almbacken drill core, Scania, Sweden.
134. Lindén, Mattias, 2001: Proglacial deformation of glaciofluvial sediments during the Pomeranian deglaciation in the Neubranden- burg area, NE Germany.
135. Warnhag, Jon, 2001: A geochemical study of the zoned Pan-African Mon Repos intrusion, Central Namibia.
136. Lundmark, Mattias, 2001: Zirkonstudie av Norra Hortens bergarter, SV Sverige.
137. Gunnarson, Rebecka, 2001: Sedimentologisk undersökning av en moränskärning i en djupvittrad sprickdal på Romeleåsen, Skåne.
138. Karlsson, Christine, 2001: Diagenetic and petrophysical properties of deeply versus moderately buried Cambrian sandstones of the Caledonian foreland, southern Sweden.
139. Eriksson, Mårten, 2001: Bedömning av föroreningsspridning kring en nedlagd bensin-station i Karlaby, sydöstra Skåne.
140. Ljung, Karl, 2001: A paleoecological study of the Pleistocene-Holocene transition in the Kap Farvel area, South Greenland.
141. Åkesson, Cecilia, 2001: Undersökning av grundvattenförhållanden i området kring Östra Vemmerlöv, Simrishamns kommun, sydöstra Skåne.
142. Bermin, J., 2001: Modelling Mössbauer spectra of biotite.